An Experimental and Numerical Study of Internally Torsional Strengthening of Box Beams Made from SCC Concrete

Roaa Hilmi Kadhim Al-Brees
Department of Construction Technology and Structural Materials, Engineering Academy, Peoples' Friendship University of Russia, Russia
rbstrhk90@gmail.com (corresponding author)

Mohamed Ibrahim Abu Mahadi
Department of Construction Technology and Structural Materials, Engineering Academy, Peoples' Friendship University of Russia, Russia
abu-makhadi-mi@rudn.ru

Alexey Semenovich Markovich
Department of Construction Technology and Structural Materials, Engineering Academy, Peoples' Friendship University of Russia, Russia
markovich-as@rudn.ru

Darya Aleksandrovna Golishevskaya
Department of Construction Technology and Structural Materials, Engineering Academy, Peoples' Friendship University of Russia, Russia
miloserdova-da@rudn.ru

Received: 21 February 2025 | Revised: 9 March 2025 | Accepted: 18 March 2025

 DOI: https://doi.org/10.48084/etasr.10671

ABSTRACT

This study investigates the torsional performance of reinforced Self-Compacting Concrete (SCC) box beams, internally strengthened with Framed Stiffening Ribs (FSRs) or Framed Steel Stiffening Ribs (FSSRs). The experiment consists of casting and testing seven beams, one reference without any reinforcement and six strengthened. The number and type of FSRs, opened or closed, are considered the main variables of the study. The experimental results indicate that adding one opened FSSR and five closed FSSRs enhances the ultimate strength of the beams by 32.71% and 122.42%, respectively. This reveals the superiority of closed FSSRs against the open ones. In addition, the percentage of increase in the ultimate torque (T_u) of the ratio closed to opened FSSRs is 9.8%, 10.3%, and 14.7% for the beam of 1, 3, and 5 FSSRs, respectively. ABAQUS software in conjunction with Finite Element Method (FEM) are used to assess the beams numerically. A robust connection is observed between the final torque and angle of twist (θ) derived from the modeled and experimental results. The mean and coefficient of variation for the ratio of FEM to experiment for T_u, are calculated to 1.038 and 2.785%, respectively. Similarly for θ, they are 0.975 and 5.555%. Therefore, the simulation of the beams can be used to study the tortional behavior of such cases with less time, effort, and cost.

Keywords-internal strengthening; torsion; box beams; Abaqus; framed steel stiffening ribs; self-compacting concrete

I. INTRODUCTION

Torsion force (T), also referred as twisting moment, torque, or torsional moment, is a rotational force that acts around the longitudinal axis of a structural member. Torsional forces in a structure can arise from either loading eccentricity or deformations caused by the continuation of structural components that intersect at an angle [1, 2].

Box girder bridges exhibit enhanced torsional stiffness and strength, and are therefore more efficient, stable, and cost-effective in comparison to open cross sections. Consequently,

in the past few decades they have been widely used in highway flyovers and modern light rail transit elevated structures. Furthermore, their easily accessible interior simplifies their maintenance. There are two formations of box girder, trapezoidal and rectangular, with the latter having a simpler construction [3, 4].

SCC is defined as a composite material that can be placed and consolidated into position solely through its own weight, without requiring any vibration. Any combination capable of flowing, filling, and resisting segregation may be classified as SCC. Moreover, SCC mitigates insufficient accessibility to prestressing tendon anchorages. It additionally reduces noise levels and health risks for personnel with portable vibrators. Having an even top surface is the only requirement [5, 6].

The Slurry Infiltration Fiber Concrete (SIFCON) was studied taking into account only the effect of torsion [7]. Specimens of (Z) form were tested using straight, crimped, and trough-shaped mild steel fibers. In SIFCON samples, the fiber content by volume fluctuated between 6% and 8% for straight fibers and remained at 6% for the rest of the categories. Fiber content of 1% was used in Fiber Reinforced Concrete (FRC) samples with linear fibers. Their aspect ratios ranged from 75 to 125. Thus, including fibers enhances torsional strength.

The influence of steel fiber and SCC was investigated on beams subjected only to torsion in [8]. Twelve specimens were tested to assess their capacity to sustain tensile stresses. They were categorized into three groups: Normal Strength Concrete (NSC), High Strength Concrete (HSC), and SCC. Compressive strength dramatically enhanced the torsional resistance of the beam. By increasing the amount of steel fibers, the ultimate load-carrying capability of the beam was also increased.

In [9], 13 samples were studied regarding the enhancement of torsional strength of composite concrete-steel beams using steel plates bolted to their shear sides. The specimens were prepared and tested purely under torsion. One was the reference beam and the other twelve had the external steel plates connected on their webs. This study investigated three variables: the steel plate's thickness and height along with the spacing between shear connectors. It was found that steel plates connected to beams enhance torsional strength behavior. The beam with steel plate height of 150 mm, thickness of 2 mm. and spacing of shear connectors of 50 mm exhibited increased cracking torque (T_{cr}) by 250% and T_u by 278%, when compared to the reference beam.

Authors in [10] reviewed the strengthening of Reinforced Concrete (RC) beams loaded with flexural, shear, and torsional loading. Carbon Fibre Reinforced Polymers (CFRP) are commonly used to strengthen RC beams. One method to address the difficulty of torsional strengthening is that of full wrapping, which is practically inapplicable. The review concluded that 45 degrees of CFRP laminates improve beams torsional strength.

The torsional behaviors of SCC beams were investigated in [11]. The beams were structured with and without reinforcement, compressive strength of concrete, spacing of transverse steel reinforcement, hollow and solid sections, amount of steel fibers, SCC, and vibrated concrete. The use of high strength SCC beams increased the T_u between 56% and 125% for the tested beam specimens compared with the normal strength SCC. In addition, the T_u of hollow SCC beams was close to the T_u of the corresponding solid normal strength SCC beams.

A new analytical method was produced in [12] to calculate the T_u and behavior to multi-cell box girder made of reinforce concrete strengthened by CFRP strips. A modified version of the Softened Truss Model (STM) was adopted. The combination of equilibrium and compatibility conditions along with the material constitutive law, which accounts for the effect of concrete and CFRP strips, resolved the torsional problems in concrete. Moreover, specific algorithms were developed to determine the torsional behaviors of the RC multi-cell box girder with or without CFRP strips. The maximum torsion capacity increased by 54.4% and 75.77% for the single and double cell box girder, respectively.

The reinforcement of SCC hollow beams with internal concrete diaphragms or bracing of steel may enhance torsional capacity. The torsional behavior of six SCC box beams reinforced with either open or closed transversal concrete diaphragms was studied in [13]. The initial beam functioned as the reference beam for the hollow part. The second and third beams were extended by two sealed and opened diaphragms, respectively. The fourth and fifth beams were strengthened with four sealed and the opened diaphragms, respectively. The sixth beam included a solid portion. The final torque increased by 43%, 61%, 89%, and 94% for the second through the fifth beam samples, respectively. The solid segment beam had a T_u enhancement of 28% for the fourth and 33% for the fifth beam. Finally, the torque of cracking increased by 57%, 29%, 100%, and 86% for the second, third, fourth, and fifth beam samples, respectively.

In [14], seven beam specimens were constructed and subjected to torsional moment testing. The fifth, sixth, and seventh samples were reinforced with one, three, and five XW-type braces. The findings revealed a 21.9%, 41.8%, and 71.6% increase for the ultimate maximum torque, and a 12.3%, 26.2%, and 32.42% for the twist angle, for the fifth, sixth, and seventh samples, respectively.

This paper will study the torsional performance of internally strengthened with FSSR RC box SCC beams.

II. EXPERIMENTAL PROGRAM

In this section, the study investigates the behavior of reinforced SCC box beams when subjected to pure torsion. This includes the recording of visible cracking load and ultimate load. In addition, θ is measured in the quarter (*QS*) and mid span (*MS*) of the test beam along with the failure mode and crack patterns. The experiment prepared seven reinforced SCC box beam specimens focusing on torsional behavior. All box beams have uniform dimensions, as illustrated in Figure 1. Moreover, longitudinal and transverse reinforcement were constructed. The strengthening of FSSRs, presented in Figure 2, can endure more than the maximum expected torsional load capacity that may occur during specimen's test.

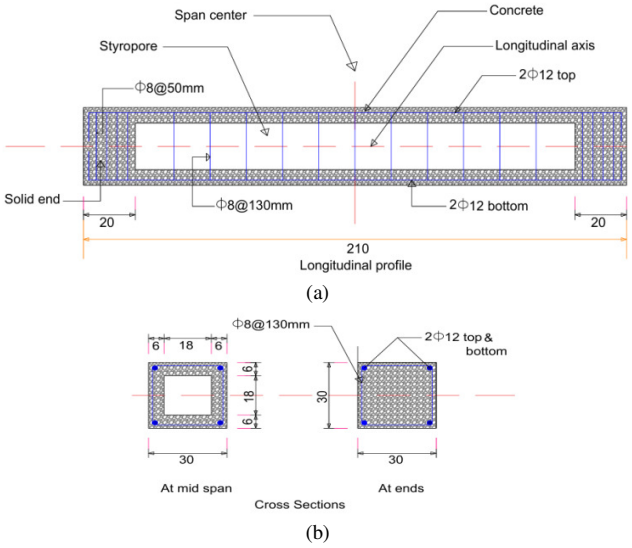

Fig. 1. Details of the tested reference beam (1NR). (a) Longitudial profile and (b) cross section.

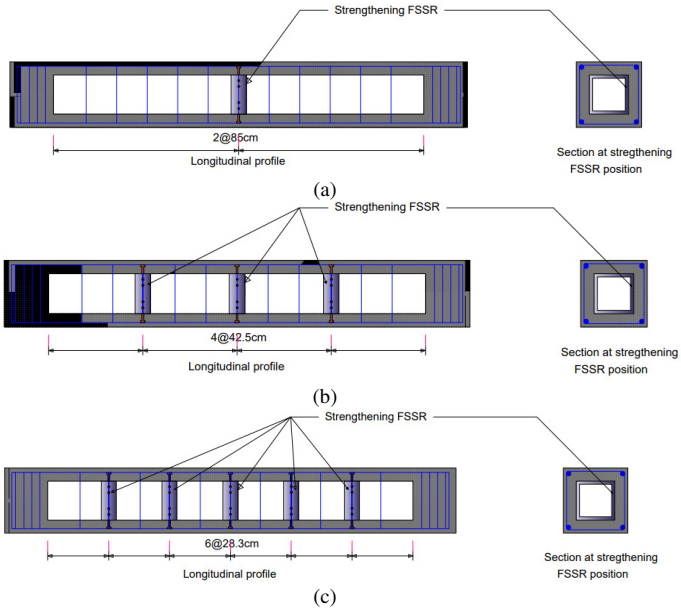

Fig. 2. Details of strengthened test beams. (a) 2N1OF or 5N1CF with one strengthening FSSR., (b) 3N3OF or 6N3CF with three strengthening FSSR, and (c) 4N5OF or 7N5CF with five strengthening FSSR.

The shear connectors, depicted in Figures 3 and 4, are constructed with headed bolts with the following specifications: a length without head of 40 mm, a head thickness of 8 mm, a diameter of 13.8 mm, a spacing of 4.5 cm, an ultimate tensile strength (*fu*) of 800 MPa, and a yield tensile stress (*fy*) of 640MPa. The quantity and type of FSSR of each beam are listed in Table I and the tensile characteristics of the steel rebars are depicted in Table II.

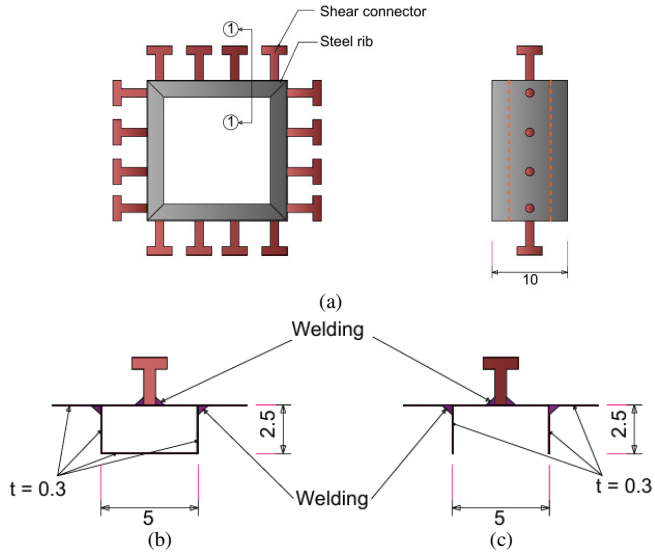

Fig. 3. FSSRs details. (a) Cross section, (b) closed section, and (c) open section.

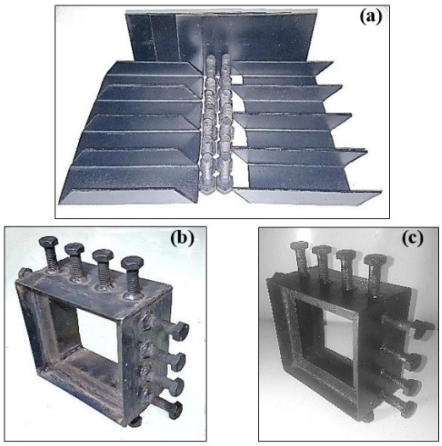

Fig. 4. FSSR details.

TABLE I. TEST BEAM DETAILS

Beam ID	FSSR quantity (No.)	FSSR Type
1NR	-	-
2N1OF	1	Opened section
3N3OF	3	Opened section
4N5OF	5	Opened section
5N1CF	1	Closed section
6N3CF	3	Closed section
7N5CF	5	Closed section

TABLE II. TENSILE CHARACTERISTICS OF STEEL REBARS

Nominal Diameter (mm)	*fy* (Mpa)	*fu* (Mpa)	Ultimate Stress Elongation (%)
8	479.6	616	11
12	565.0	709	12

Table III presents the SCC mix design and the acceptable limits according to EFNARC [15].

TABLE III. SCC MIX DESIGN

Material	Quantity	Calculated percentage	EFNARC limits
Cement (kg/m^3)	470	-	350 - 600
Sand (kg/m^3)	750	34 %	< 40%
Gravel (kg/m^3)	900	42 %	< 50 %
Silica fume (kg/m^3)	23.5	5 %	-
Limestone (kg/m^3)	130	-	-
Superplasticizers (l/m^3)	11.5	1.845 %	< 2%
Water (l/m^3)	188	-	-
W/P (%)	-	30.3 %	28 % - 38 %

The experimental setup of the study is presented in Figures 4 and 5, including the preparation and casting of the samples along with the setup utilized to test the beams.

Fig. 5. Specimen preparation and casting.

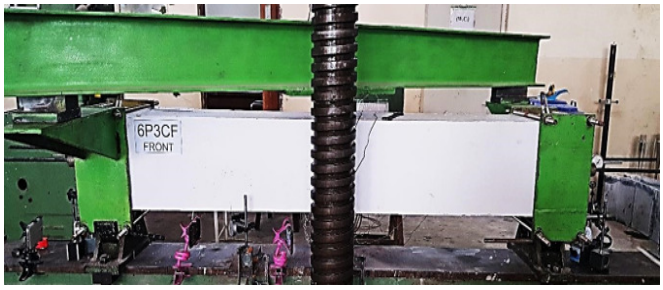

Fig. 6. Test beam setup.

III. EXPERIMENTAL RESULTS

A. Hardened Self-Compacting Concrete Properties

TABLE IV. HARDENED SCC PROPERTIES

Compressive strength (MPa)		Density (kg/m^3)	Rupture modulus (MPa)	Splitting tensile strength (MPa)	Elasticity modulus (MPa)
fc'	*fcu*				
57	57.4	2424	6.72	3	41555

B. Initial Crack Torques

The beam specimens were subjected to pure torsion with progressive stress application. The loading process persisted until the failure mechanism manifested. Both T_{cr} and T_u are presented in Table V. The higher the number of FSSRs is, the smaller is the T_{cr}/T_u ratio.

TABLE V. INITIAL CRACK TORQUES

Beam ID	T_{cr} (kN.m)	T_u (kN.m)	T_{cr}/T_u (%)	T_{cr} Increase (%)
1NR	17.51	30.64	57	Ref.
2N1OF	23.14	40.64	57	32.12
3N3OF	22.51	48.76	46	28.61
4N5OF	22.51	59.39	38	28.6 3
5N1CF	21.89	44.64	49	25.01
6N3CF	22.51	53.76	42	28.61
7N5CF	23.14	68.14	34	32.13

C. Test Beam Deformability

Deformability refers to the curvature of a section, the twist, and deflection of a member. θ is measured at four locations: the right and left ends. The average of these values is referred as θ end span (θES), the quarter span as θQS, and the middle point as θMS, all of which are listed in Table VI for all tested beams.

TABLE VI. CRACKING AND ULTIMATE TORQUE DEFORMATION

Beam ID	Deformation at T_{cr}			Deformation at T_u		
	θES (deg)	θQS (deg)	θMS (deg)	θES (deg)	θQS (deg)	θMS (deg)
1NR	0.328	0.183	0.057	3.538	2.667	1.975
2N1OF	0.441	0.200	0.063	4.358	3.501	2.964
3N3OF	0.319	0.160	0.063	4.102	3.438	2.833
4N5OF	0.218	0.103	0.052	3.908	2.913	2.581
5N1CF	0.271	0.183	0.069	3.656	3.740	3.484
6N3CF	0.275	0.258	0.103	4.054	4.657	4.845
7N5CF	0.208	0.126	0.069	3.761	3.250	3.900

Figure 6 illustrates the relationship between the applied torque and θ. The applied load leads to a linear increase in θ until reaching T_{cr} and to a nonlinear for higher values. The specimens' resistance to the applied force, prior to cracking, depends on concrete behavior leading to varied θ behavior at T_{cr}, in comparison to the reference beam. On the other hand, at Tu, θ has an inverse relationship with the number of strengthening FSSRs when compared to the reference beam. These values are higher than those of the reference beam due to the increase in torsional load capacity. This relationship is attributed to the contribution of the reinforcement to the resistance to the applied torque, for both longitudinal and transverse reinforcement.

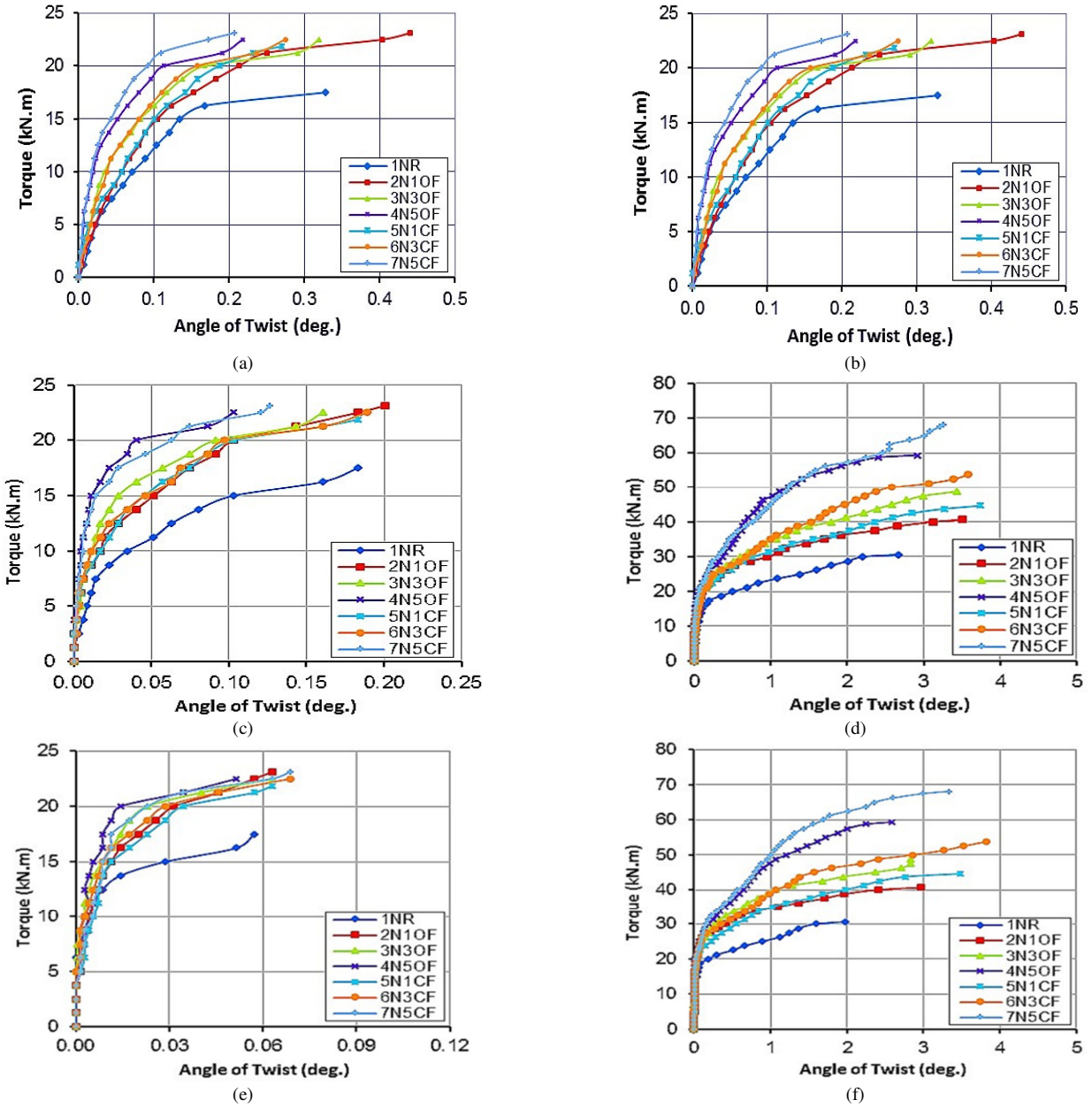

Fig. 7. Torque and θ relationship for: (a) right (ES), (b) left (ES), (c) right (QS), (d) left (QS), (e) right (MS), (f) left (MS).

D. Load-Carrying Ccapacity and Failure Mode

This part of the study presents the distribution of fractures over the length of the beam sample throughout the experiment. The first fracture is observed at MS mid-height of the front or top face of the beam, the weakest point. Thereafter, the fracture grew progressively regarding all specimens. The cracks expanded progressively in all directions as the applied torque increased, leading to a spiral configuration. Significant fractures originated and progressed inside the central third of the span and their widths are diminished closer to the end of the beam. The ultimate failure location of the majority of the beam samples was at the midpoint. All examined specimens failed due to diagonal fissures in the concrete, characterized by a spiral formation. Cracks in FSSR reinforced beams appeared less often and at a slower rate. Figure 8 illustrates the crack patterns of the test beams.

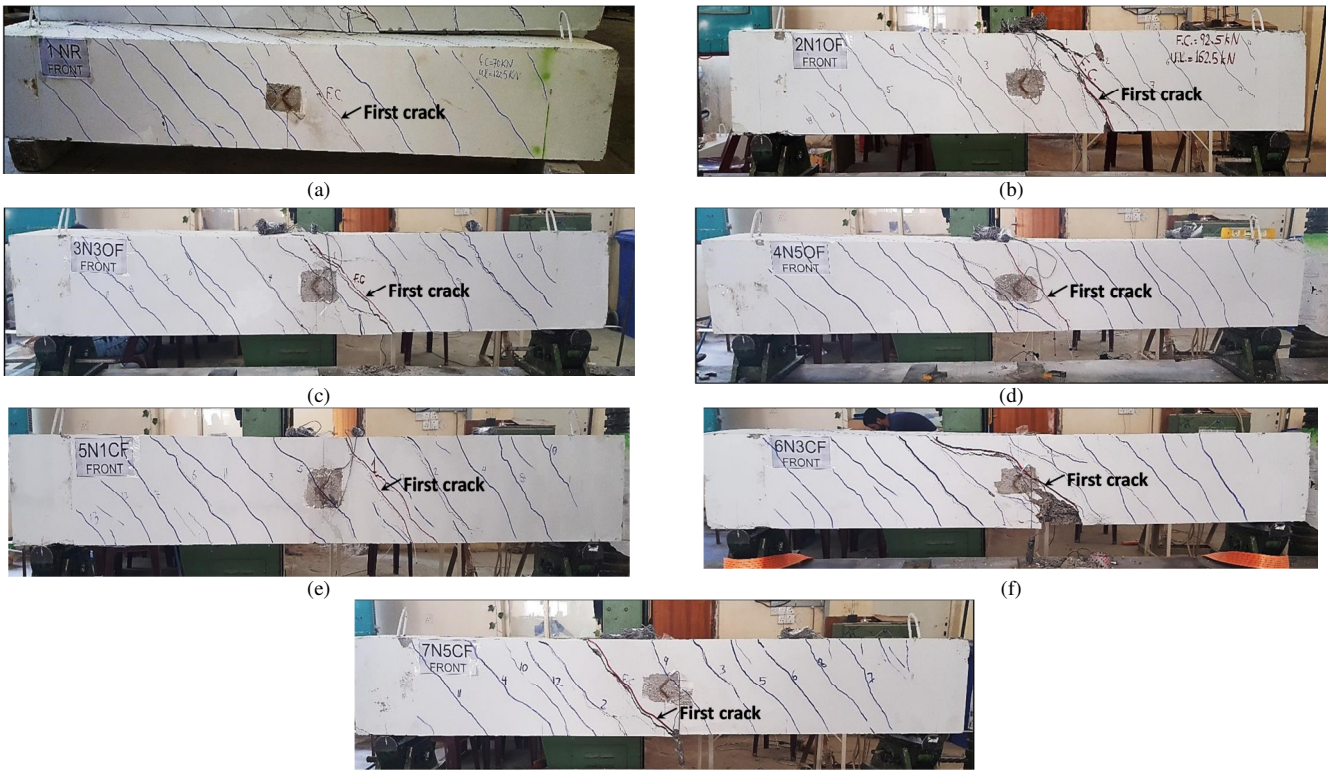

Fig. 8. Final crack patterns of specimens: (a) 1NR, (b) 2N1OF, (c) 3N3OF, (d) 4N5OF, (e) 5N1CF, (f) 6N3CF, and (g) 7N5CF.

Table VII shows the T_u for all the tested beams and compares it with the failure torque value of the reference beam. It is evident that all strengthened beams have higher T_u when compared to the reference one.

TABLE VII. BEAM ULTIMATE LOADS

Sample ID	T_u (kN.m)	T_u increase (reference) (%)	T_u increase (closed to the opened FSSRs) (%)
1NR	30.64	Ref.	-
2N1OF	40.64	32.71	-
3N3OF	48.76	59.21	-
4N5OF	59.39	93.93	-
5N1CF	44.64	45.7 2	9.8
6N3CF	53.76	75.5 1	10.3
7N5CF	68.14	122.42	14.7

1) FSSR Number Effect on T_u

The higher number of added FSSRs resulted in an enhancement of the ultimate strength by about 32.71% and 122.42% for the beam with one opened FSSR and the beam with five closed FSSRs, respectively. The number of added FSSRs is directly proportional to the beam failure torque.

2) FSSR Type Effect on T_u

The closed FSSRs exhibit superior performance compared to the opened ones. The T_u increase percentage, as shown in Table VII, is higher by 9.8%, 10.3%, and 14.7% for beams 1, 3, and 5, respectively.

IV. FINITE ELEMENT MODELING AND ANALYSIS

In order to examine the modeled beams, FEM along with the ABAQUS software are utilized [16]. To model every beam sample in the ABAQUS environment, several components are taken into account, as depicted in Figures 8(a)-8(c). The structural analysis for all beams is conducted during the static analysis step. The isoperimetric eight-node brick element (C3D8R) is used to represent the concrete beam, FSSRs, torque arm plates and bolts, prestress end plates, and strands. Each node is capable of movement along the three-dimensional x, y, and z axes. The three-dimensional two-node bar element (T3D2) was used for the bar steel and stirrups. Steel plates for reinforcement and load distribution were added to mitigate the concentration of stress at the point of loading and provide support. Moreover, the tie constraint option was also enabled to join the master concrete surface and slave steel plate surface and to eliminate any relative motion between them. Finally, to evaluate the complete interaction, the FSSRs and reinforcement are considered to be entirely embedded in concrete, as portrayed in Figure 8(d). Additionally, Figures 8(e) and 8(f) present the boundary conditions of the beam and the load definition, respectively.

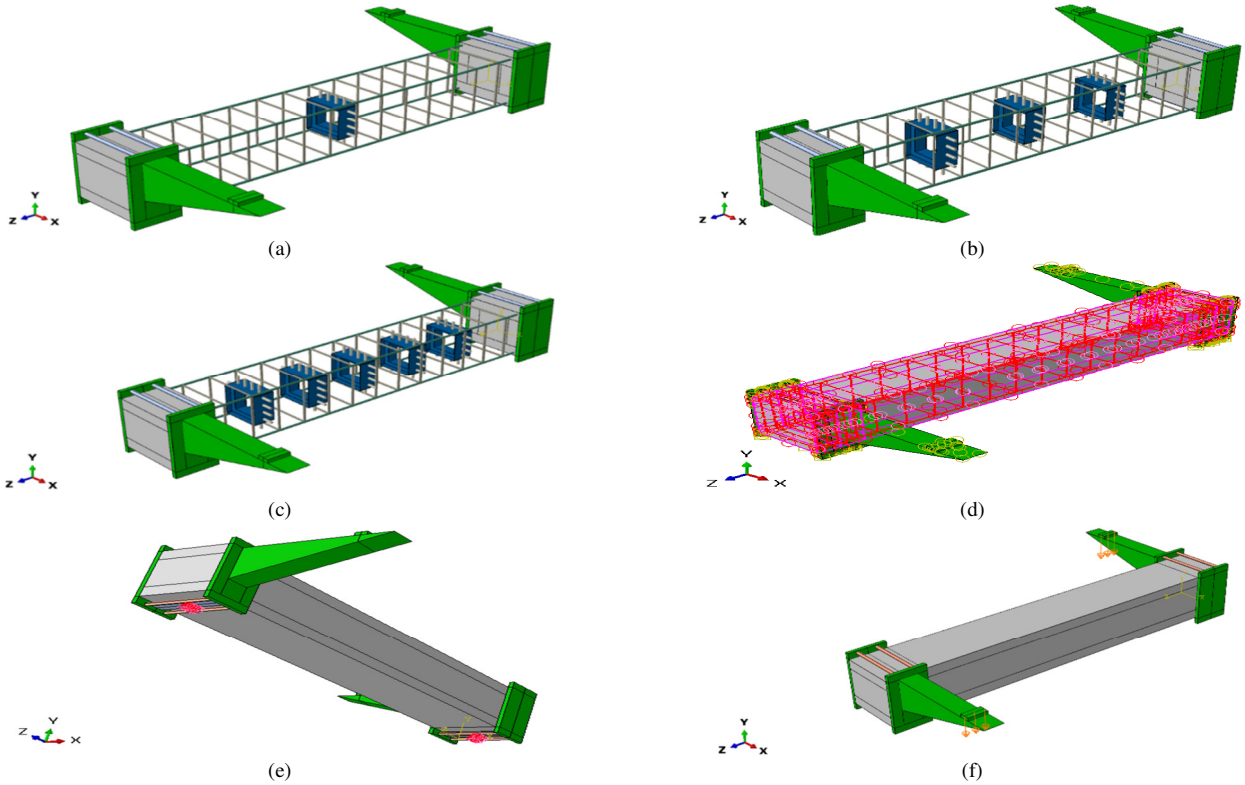

Fig. 9. (a), (b), (c) Creation and assembly, (d) embedded constraint between concrete of FSSRs and reinforcement, (e) boundary condition of the beam, and (f) load definition in ABAQUS software.

To replicate the whole performance of concrete and steel at elevated stresses, it is essential to delineate a nonlinear behavior beyond the elastic range. The damage plasticity model is used to represent the SCC. The compressive and tensile strength of SCC concrete are displayed in Tables VIII and IX, derived from the experimental findings of this work. Table X displays the input material data for the plasticity characteristics of SCC concrete. The properties of all other materials, are taken from the experimental tests presented in the previous section of this study.

TABLE VIII. SCC CONCRETE COMPRESSIVE DATA

Yield Stress (MPa)	Inelastic Strain
21.19670548	0
31.95555157	0.000101731
41.07486199	0.000222655
47.98916385	0.000404009
52.62134405	0.000645722
55.22395503	0.000951929
56.00000000	0.001307805
55.45648778	0.001669759
53.99549582	0.002064098
51.92172694	0.002473759
49.49608078	0.002889225
46.82468946	0.003317978
44.10147794	0.003746105
27.74881864	0.006686044
17.90777234	0.009485845
12.32259556	0.012149643
8.970422329	0.014719953
6.770279383	0.017302507
5.290316827	0.019849585

TABLE IX. SCC CONCRETE TENSILE DATA

Yield Stress (MPa)	Strain
2.9	0.0
2.21111	0.0660
1.216369301	0.1730
1.086699096	0.220
0.888608847	0.3080
0.811651391	0.350
0.747342963	0.390
0.690791147	0.430
0.629623921	0.480

TABLE X. SCC CONCRETE PLASTICITY DATA

Young's modulus	41555
Poisson ratios	0.20
Dilation angles	30
Eccentricities	0.10
$\epsilon_{bo}/\epsilon_{co}$	1.160
k_c	0.6670
Viscosity parameter	0.00050

Figure 10 provides a comparison of the torque and θ relationship between the experimental and numerical experiments for all beams. The computational models exhibited higher torsional stiffness when compared to the experimental data in both linear and nonlinear cases. The computer models demonstrated higher stiffness than the experimental data, across all areas.

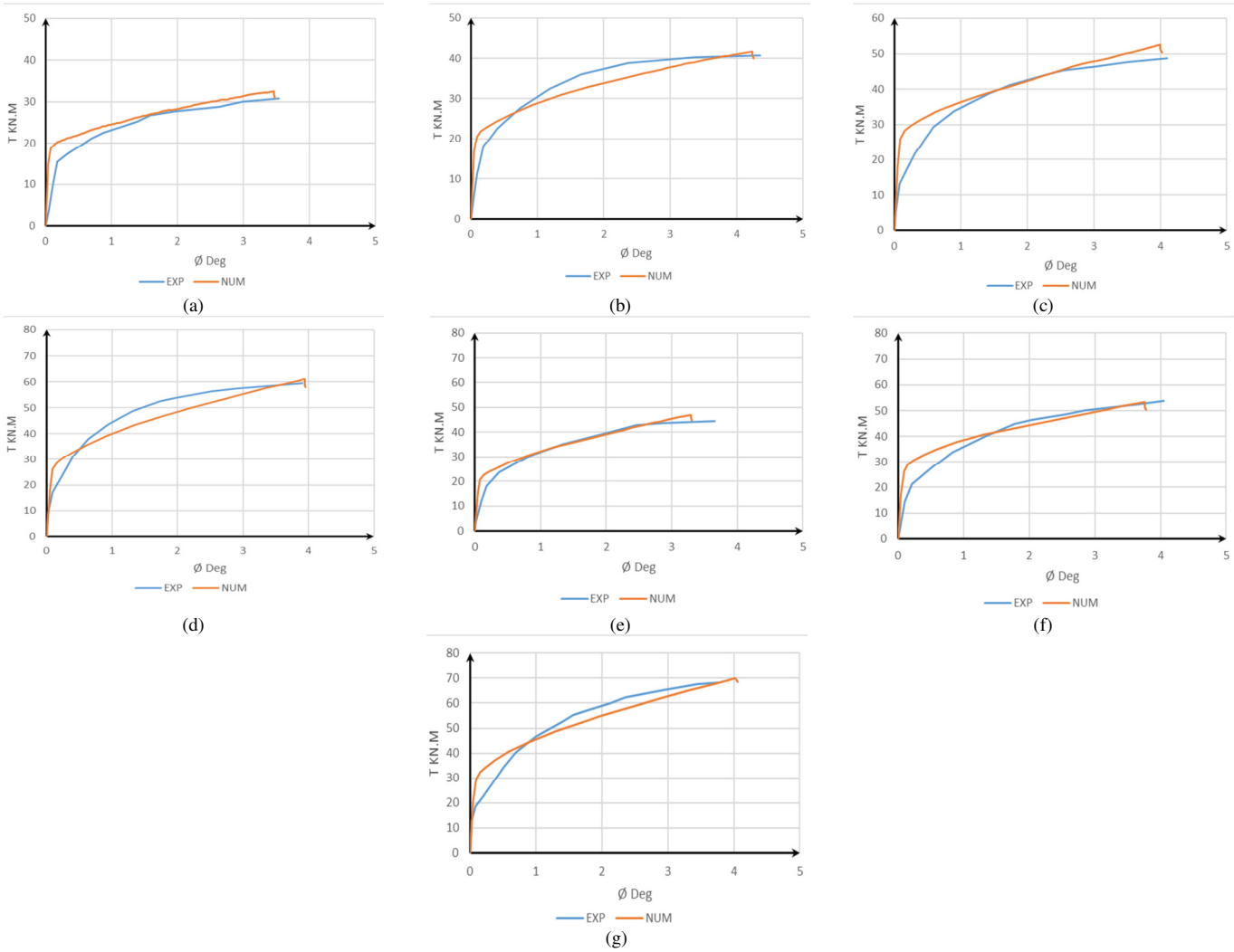

Fig. 10. Experimental and numerical torque against θ for beams: (a) 1NR, (b) 2N1OF, (c) 3N3OF, (d) 4N5OF, (e) 5N1CF, (f) 6N3CF, and (g) 7N5CF.

TABLE XI. EXPERIMENTAL AND FEM COMPARISON

Beam ID	T_u			θ at ultimate torque (θ_u)		
	EXP. (kN.m)	FEM (kN.m)	FEM/EXP	EXP. (Dig)	FEM (Dig)	FEM/EXP.
1NR	30.63	32.549	1.0626509	3.538	3.461	0.9782
2N1OF	40.63	41.666	1.0254984	4.358	4.231	0.9708
3N3OF	48.75	52.531	1.0775589	4.102	3.997	0.9744
4N5OF	59.38	61.052	1.0281576	3.908	3.939	1.0079
5N1CF	44.63	46.960	1.0522070	3.656	3.296	0.9015
6N3CF	53.75	53.255	0.9907906	4.054	3.756	0.9264
7N5CF	68.13	69.870	1.025539	3.761	4.019	1.0685

In Table XI, the failure torque is compared to θ, derived from the FEM. The experiment was conducted near the failure torque value, for all beams. The mean value of the ratio of the FEM results to the experimental (FEM/EXP.) is 1.038 and 0.975 for T_u and θ, respectively. Similarly, the coefficient of variations is 2.785% and 5.555% for T_u and θ, respectively.

V. CONCLUSION

The present study examined the torsional performance of reinforced Self-Compacting Concrete (SCC) box beams. The beams are reinforced internally with Framed Stiffening Ribs (FSRs) or Framed Steel Stiffening Ribs (FSSRs). In the experimental part of the study, SCC box beams were subjected to pure torsion, measuring visible cracking load and ultimate load. The numerical part of the study utilized ABAQUS 2019 software and Finite Element Method (FEM) to simulate the beams.

The study calculated the percentage of cracking torque (T_{cr}) to ultimate torque (T_u) capacity (T_{cr}/T_u) at 57% and 34% for the reference beam and reinforced with five FSSRs beams, respectively. This indicated that increasing the number of FSSRs reduces the T_{cr}/T_u ratio. The linear behavior of twist (θ) shifts to nonlinear when the torque exceeds T_{cr}. At T_u, a higher number of reinforced FSSRs leads to lower θ. Any beam with reinforced FSSRs remains superior to the reference due to its enhanced torsional load capacity. In addition, all analyzed specimens exhibited diagonal cracks in the concrete, displaying

a spiral pattern. Cracks in reinforced beam specimens appeared less often.

Increasing the number of added FSSRs directly enhances the ultimate strength of the beam. More specifically, the ultimate strength increased by 32.71% for the beam with one opened FSSR and 122.42% for the beam with five closed FSSRs when compared to the reference beam. This suggests that the number of added FSSRs is directly proportional to the beam failure torque. Closed FSSRs exhibited superior performance over the opened ones. The T_u increase percentage was 9.8%, 10.3%, and 14.7% for beams with 1, 3, and 5 FSSRs, respectively.

The comparison of the experimental and numerical results demonstrates a robust connection between the final torque and θ. The mean and coefficient of variation for the ratio of FEM to experiment (FEM/EXP.) are 1.038 and 2.785%, respectively for T_u. For θ they are 0.975 and 5.555%, respectively.

REFERENCES

[1] J. K. Wight and J. G. MacGrecor, *Reinforced Concrete: Mechanics and Design*, 6th ed. London , UK: Pearson Education Ltd., 2012.

[2] X. Chen, Z. Wang, X. Li, Y. Leng, K. A. Harries, and Q. Xu, "Torsional strengthening using carbon fiber reinforced polymer of reinforced concrete beams subject to combined bending, shear and torsion," *Advances in Structural Engineering*, vol. 26, no. 2, pp. 272–286, Sep. 2022, https://doi.org/10.1177/13694332221124624.

[3] M. Payoshni, K. Shilpa, and L. Savita, "Comparison of Rectangular and Trapezoidal Sections of Post Tensioned Box Girder," *International Journal of Scientific and Engineering Research*, vol. 6, no. 12, Dec. 2015.

[4] R. N. Abood and K. S. Abdul-Razzaq, "A review of previous studies on reinforced concrete box girders," *AIP Conference Proceedings*, vol. 3051, no. 1, Feb. 2024, Art. no. 100022, https://doi.org/10.1063/5.0191612.

[5] A. M. Nevile and J. J. Brooks, *Concrete Technology*, 2nd ed. London , UK: Pearson Education Ltd., 2010.

[6] N. M. Altwair, A. G. Abuzgaia, A. M. Alsharif, L. S. Sryh, S. E. A. Abdulsalam, and K. A. Swalem, "Assessing the Effects of Libyan Iron Slag on Self-Compacting Concrete Characteristics," *Engineering, Technology & Applied Science Research*, vol. 15, no. 1, pp. 19589–19595, Feb. 2025, https://doi.org/10.48084/etasr.9337.

[7] K. Balasubramanian, B. H. Bharatkumar, T. S. Krishnamoorthy, and V. S. Parameswaran, "Behaviour of SIFCON under pure torsion," *Journal of Structural Engineering (Madras)*, vol. 24, no. 1, pp. 37–40, 1997.

[8] R. H. Dakhel, "Effect of the Use of Steel Fibers and Self-compacting Concrete on the Behavior of Reinforced Concrete Beams Subjected to Pure Torsion," M.S. Dissertation, College of Engineering AL-Mustansiriyah, Baghdad, Iraq, 2012.

[9] A. A. Abdulridha, "Structural Behavior of Strengthening Reinforced Concrete Beams by Steel Plate Under Pure Torsion," M.S. Dissertation, College of Engineering AL-Mustansiriyah, Baghdad, Iraq, 2012.

[10] M. Imran, N. Shafiq, I. Akbar, and T. Ayub, "A Review of RC Beams Strengthened for Flexure, Shear and Torsion Loading," in *Proceedings of the International Conference on Civil, Offshore and Environmental Engineering*, Kuala Lumpur, Malaysia, Jun. 2012.

[11] F. A. Ra'id, "Torsional Behavior of Self-Compacting Reinforced Concrete Beams," Ph.D Dissertation, College of Engineering- AL-Mustansiriyah, Baghdad, Iraq, 2013.

[12] A. M. Abeer, A. A. Allawi, and H. K. Chai, "Theoretical Study on Torsional Strengthening of Multi-cell RC Box Girders," vol. 7, no. 2, 2013.

[13] A. Aziz and O. Hashim, "Torsional strength evaluation of reinforced SCC box beams strengthened internally by opened and closed transverse concrete diaphragms," in *Proceedings of the 3rd International Conference on Buildings, Construction and Environmental Engineering*, May 2018, vol. 162, Art. no. 04009, https://doi.org/10.1051/matecconf/201816204009.

[14] M. H. Abdallah and A. H. Aziz, "Torsional Strength Enhancement of Reinforced SCC Box Beams Using Internal Transverse Steel Bracing Technique," *International Journal of Engineering & Technology*, vol. 7, no. 4, pp. 299–306, 2018.

[15] *Specification and Guidelines for Self-Compacting Concrete,* European federation dedicated to specialist construction chemicals and concrete systems, Switzerland, 2015.

[16] *ABAQUS/Standard*. (2019), Dassault Systemes Simulia Corp.